Identification of unique and potent inhibitors of SARS-CoV-2 main protease from DNA-encoded chemical libraries

Dario Akaberi[1], Monireh Pourghasemi Lati[2], Janina Krambrich[1], Julia Berger[3], Emilia Strandback[4], Pauliina Turunen[5], Hjalmar Gullberg[6], Martin Moche[4], Praveen Kumar Chinthakindi[7], Tomas Nyman[4], Anja Sandström[7], Josef D. Järhult[8], Kristian Sandberg[9], Åke Lundkvist[1], Oscar Verho[2]*, Johan Lennerstrand[3]*

[1]*Department of Medical Biochemistry and Microbiology, Zoonosis Science Center, Uppsala University, Uppsala, Sweden*
[2]*Department of Medicinal Chemistry, Uppsala University, 75236, Uppsala, Sweden.*
[3]*Department of Medical Sciences, Clinical Microbiology, Uppsala University, Uppsala, Sweden*
[4]*Department of Medical Biochemistry and Biophysics, Protein Science Facility, Karolinska Institutet, Stockholm, Sweden.*
[5]*Science for Life Laboratory, Human Antibody Therapeutics, Drug Discovery and Development Platform, Solna, Sweden*
[6]*Science for Life Laboratory, Biochemical and Cellular Assay Facility, Drug Discovery and Development Platform, Department of Biochemistry and Biophysics, Stockholm University, Solna, Stockholm, Sweden*
[7]*The Beijer Laboratory, Department of Medicinal Chemistry, Drug Design and Discovery, Uppsala University, Uppsala, Sweden*
[8]*Department of Medical Sciences, Zoonosis Science Center, Uppsala University, Uppsala, Sweden*
[9]*Science for Life Laboratory, Drug Discovery & Development Platform, Uppsala University, Uppsala, Sweden*
[*]*Corresponding authors: Johan Lennerstrand (johan.lennerstrand@medsci.uu.se) and Oscar Verho (oscar.verho@ilk.uu.se)*

In vitro screening of large libraries of compounds with automated High-throughput screening is expensive, time consuming and requires dedicated infrastructures. Conversely, the screening of DNA-encoded chemical libraries can be rapidly performed with basic equipment available in most laboratories. In this study we identified novel inhibitors of SARS-CoV-2 main protease (Mpro) through the affinity screening of the commercially available "DELopen" library, containing 4.2 billion compounds. The identified inhibitors were peptidomimetics compounds containing a C-terminal electrophilic group able to covalently bind to M^{pro} reactive Cys145 (confirmed by x-ray crystallography). Compound SLL11 had IC50 = 30nM and was found to be well optimized, proving that the rapid exploration of large chemical spaces, enabled by DECL technology, allows the direct identification of potent inhibitors avoiding several rounds of iterative medicinal chemistry. Compound MP6, a close analogue of SLL11, showed antiviral activity against SARS-CoV-2 in the low micromolar range when tested in Caco-2 and Calu-3 (EC50 = 2.3 µM) cell lines. As peptidomimetics compounds can suffer from low cell permeability and metabolic stability, the cyclization of the compounds as well as the substitution of selected residues with D-enantiomers will be explored in the future to improve the antiviral activity of these novel compounds.

Introduction

Three years after the COVID-19 pandemic started, infections are driven by the emergence of new SARS-CoV-2 variants of concern[1]. Although mRNA vaccines have been instrumental in reducing severe disease and hospitalization, achieving long term immunity seems to be challenging and periodical boosting is required. The now dominant Omicron subvariants present over 30 mutations in the spike protein (S gene), conferring resistance to neutralizing antibodies induced by previous mRNA vaccines, bivalent vaccines or infection with a previous variant[2–4]. Also the efficacy of monoclonal antibodies used to prevent SARS-CoV-2 infection[5], disease progression and death[6,7] can be reduced by emerging variants presenting new mutations in the spike gene[6,7]. In this scenario, antiviral options for the prevention and treatment of SARS-CoV-2 infection in immunosuppressed and high-risk subjects are necessary to further reduce the COVID-19 burden. Moreover, Broad spectrum antivirals active against several coronavirus will be instrumental for preventing or mitigating the next pandemic by reducing early transmission and providing a starting point for the development of more potent compounds if necessary.

SARS-CoV-2 3-chymotrypsin-like cysteine protease (M^{pro}) also known as main protease (M^{pro})[8] mediates the maturation of viral proteins by cleaving the two viral polyproteins pp1a and pp1ab at 11 sites[9]. M^{pro} represents an attractive target for the development of antivirals against SARS-CoV-2 as it is essential for the viral life cycle and structurally conserved among alfa and beta coronaviruses[10], allowing the development of potent pan-coronavirus protease inhibitors[11–13]. The feasibility of M^{pro} inhibitors as prophylaxis or treatment against SARS-CoV-2 infection has also already been proven. Two orally administered M^{pro} inhibitors, nirmatrelvir (approved by the FDA and EMA) and ensitrelvir (approved in Japan by the Ministry of Health, Labour and Welfare (MHLW)[14] are currently approved for emergency treatment of COVID-19.

SARS-CoV-2 inhibitors have been identified through the development of substrate derived peptidomimetics[8,15] as well as screening of large libraries of compounds and fragments using different techniques like *in silico* screening[11], High-throughput screening[16] and crystallographic screening[17].

Two studies have also reported the identification of novel M^{pro} inhibitors, with IC_{50} and EC_{50} in the low micromolar range[18,19], using DNA encoded chemical libraries (DECLs). DECLs are large collections of compounds tagged with a unique DNA barcode that are screened by affinity to select binders for a target of interest[20]. Following the selection process, the chemical structures of the binders are retrieved through the sequencing of their unique DNA tags. This technology is particularly attractive because the combinatorial nature of DECL combined with affinity screening allow for the rapid and cost-efficient exploration of chemical space *in vitro*.

Here we report a new class of peptidomimetics inhibitors of M^{pro} identified using the commercially available DELopen

platform (Wuxi Apptech) that provides a library of 4.2 billion compounds (screened by the user) as well as the services necessary for the sequence to structure decoding of binders' DNA tags. The most potent compound (MP6) inhibited the activity of SARS-CoV-2 M^{pro} with IC_{50} = 24nM and SARS-CoV-2 infection with EC_{50} = 2.3 µM in cell-based assays.

Results

DNA-encoded-chemical library screening

The In vitro affinity selection of binders from DELopen library (WuXi AppTech) was performed against recombinant avi-tagged SARS-CoV-2 M^{pro} coupled to paramagnetic beads coated with streptavidin (Figure 1). The efficiency of M^{pro} coupling to the paramagnetic beads and the activity of M^{pro} bound to the magnetics beads was tested prior to the selection experiments, ensuring that the protease was stably bound to the beads while retaining its active conformation (Supplementary Figure 1 and 2). The selection of binders was performed with or without addition of SARS-CoV-2 M^{pro} inhibitors X77 (20 µM) or GC376 (5 µM) that are known to bind and block the active site of M^{pro}. Therefore, compounds selected in the presence of X77 or GC376 were regarded as possibly binding to an allosteric pocket. Selection was also performed against empty beads to identify promiscuous binders of no interest. After three rounds of selection, four highly enriched binders of which one (SLL11) was a possible allosteric inhibitor, were identified by next generation sequencing (NGS) and selected for off-DNA synthesis (NGS and synthesis of compounds were provided by WuXi Apptec).The inhibitory activity of the synthesized compounds against recombinant SARS-CoV-2 M^{pro} (Table 1) was confirmed using a FRET based enzymatic assay.The inhibitory activity of the synthesized compounds against recombinant SARS- CoV-2 M^{pro} (Table 1) was confirmed using a FRET based enzymatic assay.

Table 1: List of compounds selected from DECL libraries and relative in vitro activity.

Comp.	Enrichment score[a]				IC_{50} (µM)	
	Mpro	Mpro +X77	Mpro +GC376	Beads only	Mpro	Cathepsin S
SLL07	135654	0	0	0	0.14	> 50
SLL08	11444	0	676	0	> 50	> 50
SLL11	515485	20997	206982	0	0.030	> 50
SLL12	488354	0	0	0	0.053	> 50

[a]The enrichment score quantify how abundant a compound was after selection, e.g. a compound with enrichment score = 100 was 100 times more abundant than average

Three out of the four synthetized compounds were active with sub micromolar IC_{50} ranging from 30 to 140 nM. The two most enriched binders against M^{pro}, SLL11 and SLL12, were also the most potent (SLL11 IC_{50} = 30 nM, SLL12 IC_{50} = 53 nM) while the least enriched binder (SLL08) was not active at tested concentrations (IC_{50} > 50 µM). The active compounds displayed high selectivity for SARS-CoV-2 M^{pro} and had no off-target activity against human Cathepsin S when tested up to a concentration of 50 µM (Supplementary Figure 3). The two most potent compounds were synthesized and co-crystallized with M^{pro} to determine their binding pose and binding site (The structure of the compounds will not be disclosed before a patent application is filed).

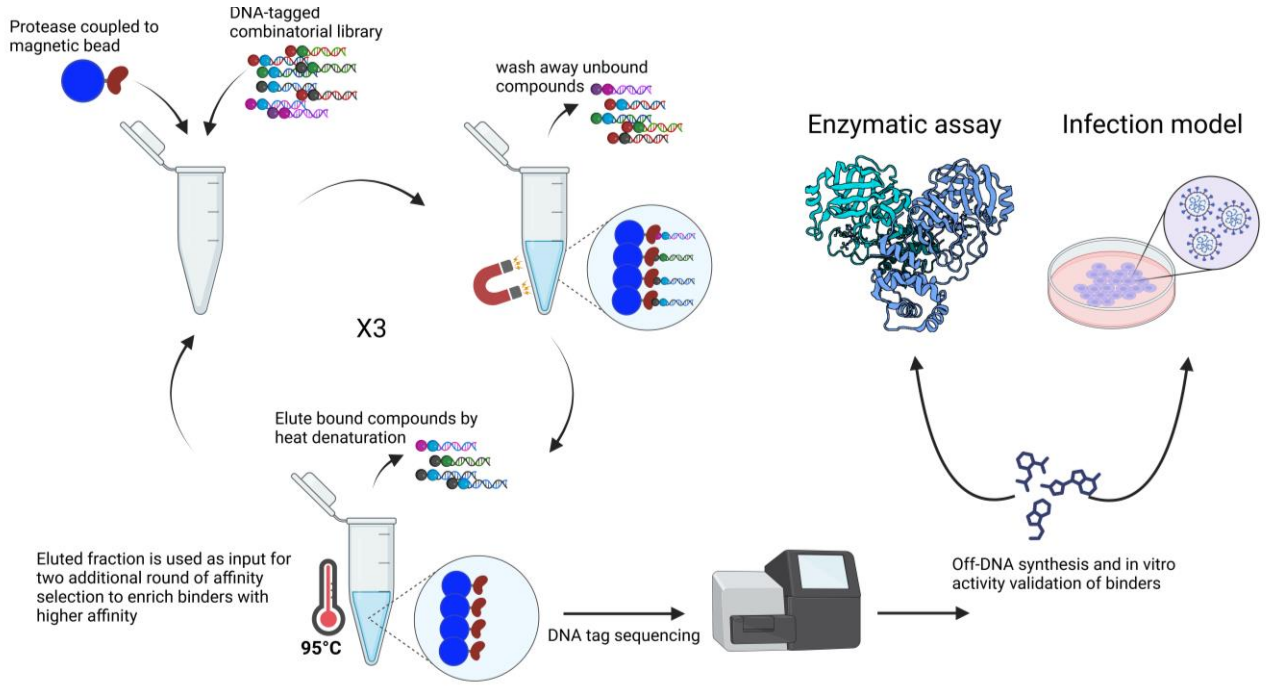

Figure 1: Overview of the project workflow. Novel inhibitors of SARS-CoV-2 Mpro were identified from the DELopen library containing 4.2 billion DNA-tagged compounds. After three rounds of affinity selection, the unique DNA-tag of binders was sequenced allowing the identification of highly enriched compounds as well as their molecular structure. Promising compounds were subsequentially synthetized off-DNA and tested to confirm their in vitro inhibitory activity against Mpro and antiviral activity against SARS-CoV-2 in cell-based assays.

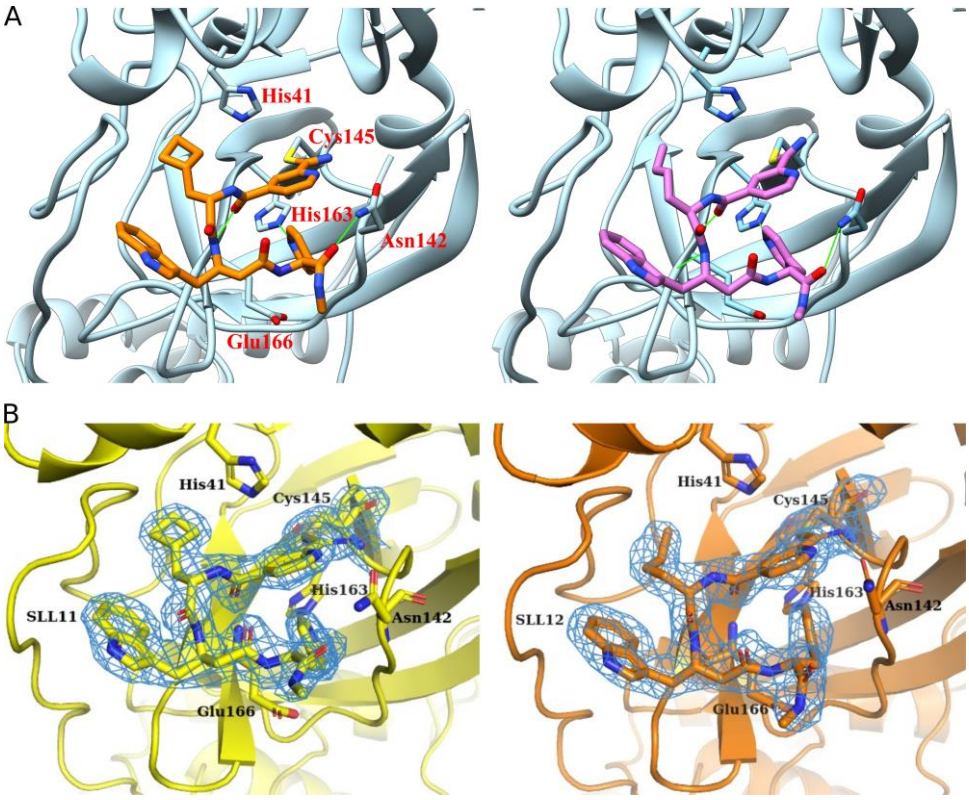

Figure 2: Compound's general structure and interactions made with sars-CoV-2 Mpro. (A) Crystal structures of compounds SLL11 (Provisory PDB ID 9EO6), shown in orange, and SLL12 (Provisory PDB ID 9EOR), shown in purple bound to SARS-CoV-2 M^{pro} active site. The two residues forming the enzyme's catalytic dyad and the residues found interacting with SLL11 are shown in red. (B) Electron density maps (2fo-fc) covering the ligands SLL11 (yellow) and SLL12 (orange) contoured at 1.2 sigma level.

SLL11 and SLL12 are peptidomimetics compounds composed of four non-natural amino acids of which P1' present an electrophilic group (Figure 2). Both compounds were found to bind to the M^{pro} active site with similar binding poses proving that SLL11 was not an allosteric inhibitor despite being selected and enriched also in presence of the M^{pro} inhibitors X77 and GC376. This was not surprising as SLL11 and SLL12 shared three out of four groups.

The compounds interacted with M^{pro} mainly via a covalent bond formed between the electrophilic P1' group and the catalytic Cys145 in the S1' subsite and a hydrogen bond formed between the P3 group and His163 in the S1 subsite. While P2 and P3 hydrophobic residues occupied the S2 and S4 subsite. Hydrogen bonds were also formed between the backbone of the compounds and Glu166 and between the N-terminal amine of SL11 and M^{pro} Asn142 side chain.

Structure activity relationship study

Compound MP6 was obtained substituting the N-terminus of compound SL11 (IC_{50} = 30 nM) with a carboxylic acid group to increase the compound solubility (Table 2). This modification caused no loss of activity, thus compound MP6 (IC_{50} = 25 nM) was used as starting point and reference for the design of analogues and comparison of inhibitory activity (Table 2). The inhibitory activity of analogues against recombinant SARS-CoV-2 M^{pro} was first screened at a concentration of 1 µM and analogues inhibiting M^{pro} activity by 80% or more were further tested to determine their IC_{50} (Dose response curves are shown in Supplementary Figure 4).

We assumed that the covalent bond formed between the C-terminal electrophilic group and Cys145 was essential for MP6 activity and started designing analogues with modification at the N-terminus of the molecule. First, analogues presenting variations of the P3 and P2 residues, were designed to assess if the size of MP6 could be reduced while retaining activity. As observed from the crystallographic binding poses, the P3 residue occupies the S2 subsite of M^{pro} and forms a hydrogen bond with His163. Therefore, removing the P3 residues (Compound MP2) or substituting P3 with groups lacking a hydrogen bond acceptor (Compounds MP7 and MP13) was poorly tolerated, reducing the compounds inhibitory activity to ~2 and ~30% respectively. Removing the side group of the P2 residue while maintaining the portion of backbone connecting P3 to the P1 residue (Compound MP4) also sharply reduced the inhibitory effect to ~8%. Since both P3 and P2 groups were essential for binding, and attempts to shorten MP6 were unsuccessful, we next assess the contribution of the P1' electrophilic group to the binding of MP6 to the active of SARS-CoV-2 M^{pro}. As expected, substituting the P1' residue with a less reactive analogue (Compounds MP5) was detrimental (~18% residual inhibitory activity) while a highly reactive aldehyde (compound MP9, IC_{50} = 24 nM) was equipotent to the original electrophile group of MP6. A bulkier electrophile group at P1' (Compounds MP22) also reduced the inhibitory activity against M^{pro} to ~ 18%. Lastly,

the analogues MP16, MP17 and MP3 were designed to evaluate variants of the P1 residues.

Table 2: List of MP6 analogues and relative Inhibitory activity against SARS-CoV-2 M^{pro}

Compound	M^{pro} Inhibition %[a] (Comp. conc. 1µM)	IC50 ± SEM (µM)[b]
MP6	97% ± 4.9 SD	0.025 ± 0.001
MP2	2.2%	n.d.
MP4	8.1%	n.d.
MP5	17.8%	n.d.
MP7	30.4%	n.d.
MP9	100%	0.024 ± 0.0004
MP13	38% ± 16.2 SD	n.d.
MP16	95.7% ± 1.3 SD	0.071 ± 0.007
MP17	90.7% ± 1.6 SD	0.069 ± 0.004
MP22	18.2%	n.d.
MP3	86.6% ± 1.1 SD	0.139 ± 0.049
MP12	96.5% ± 4.5 SD	0.106 ± 7[c]
MP18	94.2% ± 5.7 SD	0.047 ± 0.006
MP19	98.2% ± 2.6 SD	0.045 ± 0.009
MP20	66.8%	n.d.
MP21	94.7% ± 3.4 SD	0.033 ± 0.003

[a] Compounds were tested at concentration of 1 µM with triplicates (n = 3 replicates). Average inhibition of Mpro ± standard deviation (SD) is shown only for compounds that were tested in two independent experiments.

[b] Average IC_{50} and standard error of the mean (SEM) were calculated from two independent experiments where each compound's concentration was tested in triplicates (n = 3 replicates).

[c] The IC_{50} of compounds MP12 was determined from a single experiment where each compound's concentration was tested in triplicates (n = 3 replicates), standard deviation (SD) is reported instead of SEM.

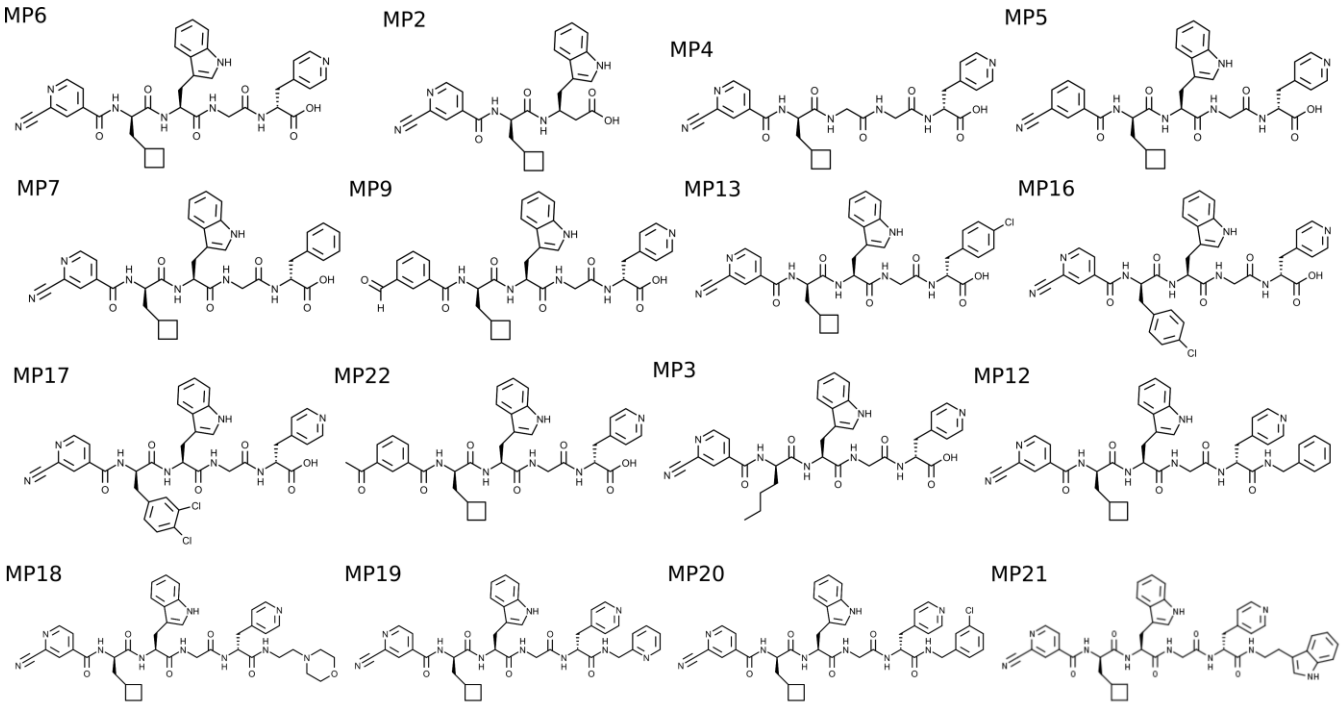

Exchanging the hydrophobic P1 group to other hydrophobic aliphatic (MP3 IC_{50} = 139 nM) or planar aromatic groups (MP16 IC_{50} = 71 nM and MP17 IC_{50} = 69 nM) reduced the IC_{50} of the analogues up to 4-fold. However, all the analogues maintained sub micromolar activity with IC_{50} in the low nanomolar range.

Overall, all residues constituting MP6 seemed to be well optimized, so we explored the addition of a fifth residue at the N-terminus of MP6. Analogue with a polar P4 residues (Compounds MP18 IC_{50} = 47 nM, MP19 IC_{50} = 45 nM and MP21 IC_{50} = 47 nM) were ~2 fold more potent than analogue with a non-polar P4 residues (MP12 IC_{50} = 106 nm), suggesting that the P4 residues might take part in hydrogen bonding with residues located near the S1 subsite of M^{pro}.

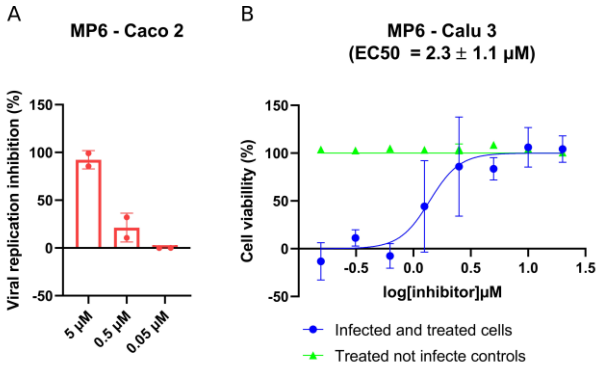

Figure 3: Antiviral effect of MP6 against SARS-CoV-2. (A) The Inhibitory effect on viral replication was assessed using a yield reduction assay. Caco-2 cells were infected with SARS-CoV-2 (MOI 0.01) and treated with 5, 0.5 or 0.05 µM of MP6. Supernatants were collected 48h post infection and viral copy number per ml were quantified by RT-qPCR. The reduction in viral copy number per ml from two independent experiments is reported as inhibition of viral replication (%) ± SD. (B) Inhibitory effect on CPE development induced by SARS-CoV-2 infection. Calu-3 cells were infected (MOI 0.01) and treated with different concentrations of MP6, 48h post infection cell viability was assessed by MTT assay. The average EC50 from two independent experiments is reported ± the standard error of the mean.

Antiviral activity of MP6 against SARS-CoV-2 in cell-based assays

MP6 was chosen to test the antiviral activity of the novel scaffold discovered in this study. The compound cell permeability was first evaluated Caco-2 cells (human colon epithelial cells) that were cultured on a permeable filter. MP6 showed good apical to basolateral (A-B) permeability (*P*app A-B = 5.4 x 10^6 ± 3.6 x 10^6 cm/s) and lower basolateral to apical (B-A) permeability (*P*app B-A = 2.5 x 10^6 ± 0.6 x 10^7 cm/s) with no observable efflux of the compound (*P*app B-A / *P*app A-B = 0.5). Accordingly, MP6 was active in Caco-2 cells and showed dose response inhibition of the viral replication measured by RT-qPCR (Figure 3A). Since Caco-2 cells are highly permissive for SARS-CoV-2 infection but do not develop CPE, we tested the capacity of MP6 to inhibit CPE development and increase cell viability in infected Calu-3 cells (Human lung epithelial cells). Unexpectedly, MP6 had no protective effect in infected Calu-3 at concentrations as high as 20 uM (data not shown). Based on previous studies reporting the P-glycoprotein (P-gp) mediated efflux of M^{pro} peptidomimetics inhibitors [12,21,22], we assumed MP6 being a substrate of P-gp. When tested in combination with the P-gp inhibitor CP-100356 (4 µM), MP6 showed dose dependent inhibition of CPE development with EC_{50} = 2.3 ± 1.1 µM and observable cytotoxic effect (Fig. 2B).

Effect of the E166V M^{pro} variant on MP9 inhibitory activity

The inhibitory activity of MP9 was tested against recombinant M^{pro} carrying the E166V (M^{pro}-E166V) variant, known to confer resistance against nirmatrelvir. MP9 and nirmatrelvir had comparable IC_{50} in the low nanomolar range against the recombinant wild type M^{pro} (M^{pro}-WT). The inhibitory activity of both compounds was significantly decreased to 15.7 µM (nirmatrelvir) and 21.1 µM (MP6) against M^{pro}-E166V (Figure 4).

Discussion

In this study we report the identification of novel inhibitors of SARS-COV-2 M^{pro} from the commercially available "DELopen" DNA encoded chemical library (DECL).

Three potent compounds (SLL07, SL11 and SLL12) with IC_{50} in the low nanomolar range were directly identified through the cost-efficient affinity screening of 4.2 billion combinatorial molecules. The selected compounds were peptidomimetic formed by four unnatural amino acids with a reactive electrophilic group at the C-terminus. Crystallographic studies of SLL11 and SLL12 binding poses showed that side groups of all four residues (P1', P1, P2 and P3) occupied one of the major subsites of M^{pro} active site (S1', S1, S2 and S4) with a novel arrangement of the peptidomimetics backbone to fit the binding site.

Attempts to further improved the compounds' potency by systematically varying one of the four unnatural residues resulted in the design of several analogues with IC_{50} lower than 100nM. However, SLL11 (and its close analogue MP6) remained the most potent inhibitor (IC_{50} = ≤ 30nM) proving that the screening of large combinatorial libraries can identify well optimized compounds without the need for several iterative cycles of medicinal chemistry.

Reducing the molecular weight thus improving the physiochemical properties of the compounds proved to be difficult. The inhibitory activity of analogues with a less reactive electrophile at P1' was almost completely abrogated, suggesting that a covalent interaction with M^{pro} was essential. Co-crystallization of SLL11 and SLL12 with SARS-CoV-2 M^{pro} confirmed that the C-terminal electrophilic group formed a covalent bond with Cys145 of enzyme's catalytic dyad as reported for several other peptidomimetic inhibitors of M^{pro}[12,22–24]. Likewise, removing the whole P2 residue or P3 side group was not possible without causing a drop in compounds inhibitory activity. P3 formed an essential hydrogen bond with S2 His163 that mimics the interaction with the glutamine residue of its natural substrate[25]. The side group of the P2

residue did not form any hydrogen bond with residues in the S4 pocket but was still essential for activity, suggesting that P2 contributes with more than just connecting P3 to the remaining part of the molecule.

When tested in cell-based assays, MP6 showed antiviral activity against SARS-CoV-2 in the low micromolar range in both Caco-2 and Calu-3 (EC_{50} = 2.3 ± 1.1 µM), two cell lines commonly used as infection model for SARS-CoV-2. However, while no efflux was observed in Caco-2 permeability test, the addition CP-100356 was necessary to prevent MP6 efflux mediated by P-glycoprotein (P-gp) in Calu-3 cells. This finding supports a previous report of Calu-3 cells expressing P-gp at higher level than to Caco-2 cells[26]. The relatively low activity of MP6 in cell-based assay could be explained by the compound's sensitivity to proteolytic degradation as both SLL11 and SLL12 showed low metabolic stability in human and mouse microsomes (supplementary Table 1). Cyclization or substitution of selected residues with D-enantiomers are two strategies that could improve the metabolic stability of the peptidomimetics reported in this study and will be subject of further studies in our lab.

Finally, the in vitro inhibitory activity of MP9 was evaluated against recombinant M^{pro} carrying the variant E166V that cause high fold resistance to nirmatrelvir[27–29]. The E166V mutant conferred 811-fold resistance to MP9 and 523-fold resistance to nirmatrelvir in our FRET based enzymatic assay. The observed increase in nirmatrelvir's IC_{50} against SARS-CoV-2 M^{pro} was comparable to the 473-fold increase reported by Lan et al. in a similar enzymatic assay[28]. The dramatic effect of E166V mutation on nirmatrelvir activity was shown to be due to steric clashes in S1 preventing the formation of hydrogen bonds between nirmatrelvir's γ-lactam ring, residues HIS51 and possibly also ASP166 itself or PHE140. As a result of the disrupted key interaction in S1, the nitrile warhead is moved out of position making it more difficult to interact with CYS145[28,29].

MP9 also interacts with residue HIS51 trough hydrogen and CYS145 with its aldehyde warhead. at P1', the effect of the E166V variant on the activity of MP6 and other analogues will be assessed.

It is therefore plausible that similar dynamics are the cause of MP9 reduced activity observed *in vitro*. Although the only difference between MP6 and MP9 is the warhead group

Material and methods

Bead capture test

Immobilization of M^{pro}-Avi to Dynabeads MyOne Streptavidin T1 paramagnetic beads was tested before affinity selection according to a protocol provided with the DELopen kit. All reagents were added to 1.5 ml Epperdorf DNA Low Binding tubes during bead capture test and affinity selection. In brief, paramagnetic beads were washed three times with 1X wash buffer (50 mM Tris-HCl pH 7.5 – 150 mM sodium chloride – 0.05% Tween-20 – 1 mM dithiothreitol) using DynaMag-2 magnetic stand (Invitrogen). M^{pro}-Avi (6 ug) was diluted to 1X selection buffer (50 mM Tris-HCl pH 7.5 – 150 mM sodium chloride – 0.05% Tween-20 – 1 mM dithiothreitol - 0.1 mg/ml sheared salmon sperm DNA) and an aliquot was collected as input sample. Remaining Avi-tagged protein (5 ug) was immobilized to Dynabeads MyOne Streptavidin T1 paramagnetic beads at room temperature for 30 minutes. Flowthrough was collected and beads were washed once with selection buffer. Beads were suspended to 1X selection buffer, a 'beads' sample was collected, and the remaining bead suspension was heated at 95° C for 10 minutes. Beads were collected using a magnetic stand and solution was collected as heated eluate sample. Beads were resuspended to selection buffer (heated beads). To visualize the relative amount of immobilized and eluted protein the bead capture test samples were separated by SDS-PAGE. Samples were denatured and reduced using NuPAGE LDS Sample Buffer (4X) (Invitrogen) and NuPAGE Sample Reducing Agent (10X) (Invitrogen) by heating at 95° C for 5 minutes. Samples were separated on NuPAGE 4-12% Bis-Tris Mini Protein Gels (Invitrogen) using matched electrophoresis run chamber at 200V for 35 minutes. Proteins on the gels were visualized using InstantBlue Coomassie Protein Stain (Abcam), destaining with distilled water.

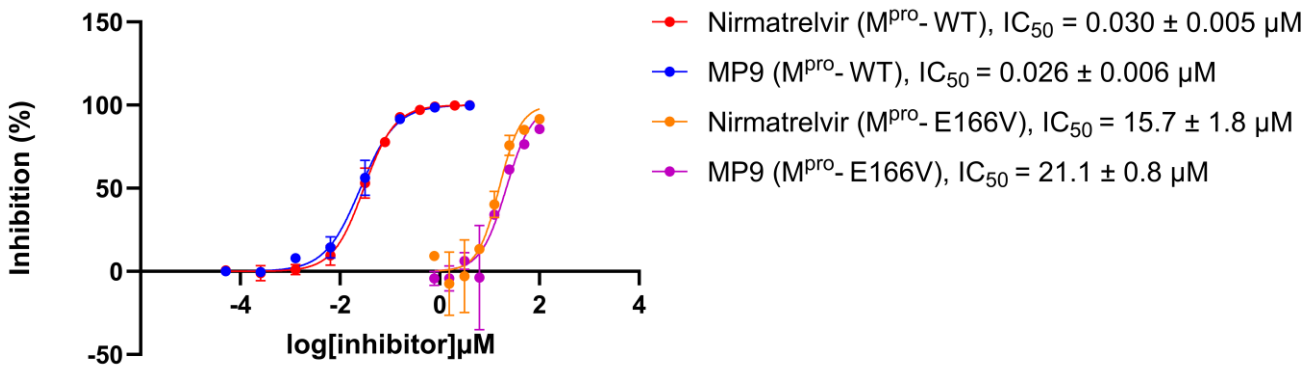

Figure 4: Effect of the E166V variant on the inhibitory activity of MP9 and nirmatrelvir. Dose response curves of MP9 and nirmatrelvir tested against recombinants wild type (Mpro-WT) and mutated Mpro carrying the E166V (Mpro-E166V). IC_{50} values are reported as average ± SEM from two independent experiments perfumed with triplicates.

DECL affinity selection

Three rounds of affinity selection were performed using the 3rd generation DELopen DECL (WuXi Apptec; hits.wuxiapptec.com/delopen) according to the provider's instructions. Before each round, M^{pro}-Avi (5 ug) was immobilized to Dynabeads MyOne Streptavidin T1 paramagnetic beads at room temperature for 30 minutes in 1X selection buffer. Reversible small molecule inhibitors were added at 20 µM concentration for the last 10 minutes of immobilization and included into DEL incubation mixtures at 20 µM final concentration. Covalent inhibitors at 5 µM were preincubated with immobilized target for 10 minutes at room temperature but not added to the DEL incubation. Bead-immobilized target at final concentration 1.7 µM was incubated with the DELopen compound library in 1X selection buffer (50 mM Tris-HCl pH 7.5 – 150 mM sodium chloride – 0.05% Tween-20 – 1 mM dithiothreitol - 0.1 mg/ml sheared salmon sperm DNA) for one hour at room temperature with gentle rotation. Three wash cycles were performed with 1X selection buffer (50 mM Tris-HCl pH 7.5 – 150 mM sodium chloride – 0.05% Tween-20 – 1 mM dithiothreitol) after each round. The compound release method was heating for 10 minutes at 98°C after each round. Samples collected after the third selection round were stored at -80°C before transfer to Wuxi App Tec for post-selection quality control and deep-sequencing.

Protease expression and purification

SARS-CoV-2 3CL protease (M^{pro}) was produced as previously described[30]. The used construct contained nucleotide sequences corresponding to SARS-CoV-2 M^{pro} residues S1-Q306 (Chinese isolate, NCBI accession number YP_009725301). A detailed protocol is provided in the supporting information.

Protease expression and purification

Avi-tagged SARS-CoV-2 M^{pro} protease was kindly provided by Anders Olsson, SciLifeLab Stockholm. A detail protocol for the expression and purification of the enzyme is provided in the supporting information.

In vitro enzymatic assay:

All experiments were carried out as previously reported[30] in black flat-bottomed 96 well plates (Nunc, Thermo Fisher Scientific) in a final volume of 100 µl. Different concentrations of the compounds were incubated with recombinant SARS-CoV-2 protease (final concentration 100nM) in assay buffer (20 mM HEPES pH 7.5, 0.01% Triton X-100) for 10 minutes at room temperature. The enzymatic reaction was started by adding the substrate DABCYL-Lys-Thr-Ser-Ala-Val-Leu-Gln-Ser-Gly-Phe-Arg-Lys-Met-Glu-EDANS at a final concentration of 20 µM. The fluorescent emission was monitored every 60 seconds for 40 minutes using Tecan infinite M200 PRO plate reader (Tecan Trading AG, Switzerland) with the excitation wavelength set to 355 nm and the emission wavelength set to 538 nm.

For the initial screening, compounds stocks (10mM in 100% DMSO) were diluted to 10µM in assay buffer and then further diluted ten time to the final concentration of 1 µM by transferring 10µl in the assay wells (final volume 100 µl). The final concentration of DMSO was kept to 0.01% (v/v) in all wells comprising the controls wells, all compounds and controls were tested with triplicates.

For the SAR study, compound's IC_{50} were determined with a 12-points concentration series composed of one series of six 1:5 dilutions ranging from 4 to 0.00128 µM (final concentration in the well), and a second series of six 1:5 dilutions ranging from 2 to 0.00064 µM (final concentration in the well). Average IC_{50} and standard error of the means were calculated from two independent experiments with each compound concentration tested in triplicates. DMSO concentrations were always kept ≤ 0.04% (v/v) in all wells.

For resistance testing, nirmatrelvir and MP9 compounds were tested at final concentration ranging from 4 µM to 0.00005 µM (eight 1:5 serial dilutions). The recombinant SARS-CoV-2 M^{pro}, Washington strain, (WA1, accession number MT246667) carrying the E166V mutation was used at a final concentration of 500nM. The WT M^{pro} also from the WA1 strain was used for comparison. Average IC_{50} and standard error of the means were calculated from two independent experiments with each compound concentration tested in triplicates. DMSO concentrations were always kept ≤ 0.04% (v/v) in all wells.

The relative fluorescence units (RFU) per second were plotted and the initial velocities were calculated, normalized to the controls (untreated protease controls wells = 0% inhibition, control wells with no substrate = 100% inhibition) and expressed as % of enzyme activity inhibition. The half maximal inhibitory concentration (IC_{50}) was calculated by nonlinear regression fitting of the normalized 12-point dose response curve to the model "log(inhibitor) vs. normalized response – Variable slope" with equation: Y=100/(1+10^((LogIC50-X)*HillSlope)).
The data analysis was conducted in GraphPad Prism (v.9.5.1). (GraphPad Software, La Jolla California, USA).

CPE-based antiviral assay:

Calu-3 cells were grown in DMEM (Gibco, 41966029) supplemented with 10% FBS (Gibco, 10500064) and 1× penicillin-streptomycin (Sigma-Aldrich, PA333) and incubated at 37°C, 5% CO 2 atmosphere. The compound MP6 was tested at concentrations ranging from 20 to 0.156 µM (eight 1:2 serial dilutions). MP6 was tested in two independent experiments with each concentration tested in triplicates.

One day prior to the assay, Calu-3 cells were seeded at a density of 20.000 cells/well in a 96 wells plate in a final volume of 100µl of cell media (DMEM supplemented with 2% FBS, 1× penicillin−streptomycin, from now on referred to as DMEM-2). After overnight incubation (37°C, 5% CO_2 atmosphere), cells were pretreated for two hours with 100µl of DMEM-2 with CP-100356 (MedChemExpress, HY-108347) added at a final concentration of 4µM. After two hours, the cell media containing CP-100356 was discarded, cells were washed with 100µl of PBS and infected with 200 plaque forming unites of SARS-CoV-2 (Isolate from Sweden [31]) corresponding to a MOI ~ 0.01. After one hour the cell media with the virus was discarded, cells were washed with 100µl of PBS and treated by adding 100µl of DMEM-2 containing different concentrations of MP6 and CP-100356 at a final concentration of 4µM. After 48h, the cell media supplemented with MP6 and CP-100356 was substituted with 100µl of fresh DMEM-2 to which 10 ul of a 5 mg/mL MTT (Sigma-Aldrich, M2128) solution in PBS was added. Following 4h of incubation, formazan crystals were solubilized overnight by adding 100 ul of a 10% SDS, 0.01 M HCl solution. Optical density (OD) at 570 and 690 nm was read using a Tecan infinite M200 PRO plate reader (Tecan Trading AG, Switzerland). Throughout the assay, cell controls (not infected cells treated or not treated with MP6 at different concentrations) and infection controls (wells not treated with MP6 at different concentrations) were also treated with CP-100356 (4µM) and DMSO concentration was kept constant to 0.25% (v/v) in all wells. OD readings at different wavelengths were subtracted, the resulting values were normalized to the controls, and EC50 were determined by nonlinear regression analysis using GraphPad Prism vr.9.5 (GraphPad Software, La Jolla California, USA).

Virus yield reduction assay:

Caco-2 cells were grown in DMEM (Gibco, 41966029) supplemented with 10% FBS (Gibco, 10500064) and 1× penicillin-streptomycin (Sigma-Aldrich, PA333) and incubated at 37°C, 5% CO 2 atmosphere. The compound MP6 was tested at 5, 0.5 and 0.05 µM (eight 1:2 serial dilutions). MP6 was tested in two independent experiments with each concentration tested in triplicates.
One day prior to the assay, Caco-2 cells were seeded at a density of 20.000 cells/well in a 96 wells plate in a final volume of 100µl of cell media (DMEM supplemented with 2% FBS, 1× penicillin−streptomycin). After overnight incubation (37°C, 5% CO_2 atmosphere), cells were infected with 200 plaque forming unites of SARS-CoV-2 (Isolate from Sweden[31] corresponding to a MOI ~ 0.01. After one hour the cell media with the virus was discarded, cells were washed with 100µl of PBS and treated by adding 100µl of cell media (DMEM supplemented with 2% FBS, 1× penicillin−streptomycin) containing MP6 at different concentrations. After 48h, supernatants were collected (100ul) and mixed with 300ul of TRIzol LS (Invitrogen, ThermoFisher Scientific, Waltham, MA). The viral RNA was extracted using the Direct-zol-96 RNA Kit (Zymo Research, Irvine, CA) according to the manufacturer's protocol. The extracted viral RNA was quantified by RT-qPCR using primers (Thermo Fisher Scientific, Waltham, MA) previously described[32] and the SuperScript III OneStep RT-PCR System with Platinum Taq DNA Polymerase kit (Invitrogen, Thermo Fisher Scientific, Waltham, MA). Target E: forward primer 5′-ACAGGTACGTTAATAGTTAATAGCGT-3′; reverse primer 5′ GTGTGCGTACTGCTGCAATAT-3′; and the probe 5′-FAM-CACTAGCCATCCTTACTGCGCTTCG-TAMRA-3′. The reaction mixture contained 12.5 ul of reaction buffer (a buffer containing 0.4 mM of each dNTP, 3.2 mM MgSO4), 0.5 ul of SuperScript III RT/Platinum Taq Mix, 0.5 ul of each primer (10 µM (µM) stock concentrations), 0.25 ul probe (10 µM stock concentration), 2.4 ul of 25 mM magnesium sulfate, 3.35 ul of nuclease-free water, and 5 ul of RNA template. The RT-qPCR assay was performed on a CFX96 Touch Real-Time PCR Detection System (Bio-Rad Laboratories, Hercules CA) under the following conditions: reverse transcription at 55 °C for 30 min and 95 °C for 3 min, followed by 45 cycles of denaturation at 95 °C for 15 s, extension at 57 °C for 30 s, and collecting the fluorescence signal at 68 °C for 30s.
All samples were run in triplicate. The corresponding number of copies for each Ct was calculated from a standard curve prepared with synthetic DNA gene fragments (gBLOCKs; IDT, San Jose, CA) with a five-base-pair deletion in the amplified regions of the viral genome diluted in deionized, nuclease-free water to concentrations of 103–105 copies per ul. The five-base-pairs were deleted to be able to distinguish between viral RNA and gBLOCKs during sequencing. The LODs for both genes were 101 copies per ul. The relative fluorescence unit (RFU) data were obtained from the CFX Maestro Software (Bio-Rad CFX Maestro for Mac 1.1 Version 4.1.2434.0214, Bio-Rad Laboratories, Hercules, CA). Quantified viral RNA from infected wells treated with different concentrations of the compounds were normalized to the controls using GraphPad Prism vr.9.5 (GraphPad Software, La Jolla CA).

Compounds synthesis:

All compounds were synthesized by a solid-phase peptide synthesis (SPPS) strategy on 2-chlorotrityl chloride resin (2CTC) using various Fmoc-protected natural and unnatural amino acids. All compounds prepared were either dipeptides or tripeptides terminated by a carboxylic acid as capping agent at the N-terminus. Below follows, a general synthetic procedure describing the preparation of a carboxylic acid capped tripeptide; however, the corresponding capped dipeptides can be obtained in an analogous fashion by carrying out one less amino acid coupling.
To a 3 mL syringe with a frit was added 2CTC resin (63 mg, 0.1 mmol, 1 equiv.), after which a solution of Fmoc-protected amino acid #1 (0.2 mmol, 2 equiv.) and *N*,*N*-diisopropylethylamine (DIPEA, 0.05 ml, 0,30 mmol, 3 equiv.) in dichloromethane (DCM, 1 ml) was prepared, and subsequently aspirated into the syringe. The resulting

mixture was agitated at room temperature for 2 h to allow for coupling of amino acid #1 to the resin, after which the reaction solution was ejected and the 2CTC resin was washed with dimethyl formamide (DMF, 2x1 ml) under agitation for 30 seconds. To deactivate the remaining 2CTC functionalities on the resin, a solution of DCM/Methanol/DIPEA (ratio 85:15:5, 1.05 mL) was aspirated into the syringe and it was agitated for an additional 15 minutes. Following this, the 2CTC resin was washed with DMF (2x1 ml) and DCM (3x1 ml), before being subjected to subsequent Fmoc deprotection. Removal of the Fmoc group was accomplished by treating the 2CTC resin with piperidine in methanol (80%, 1 ml) for 20 min under agitation at room temperature. The reaction solution was then ejected from the syringe, and the 2CTC resin was carefully washed using DMF (3x1 ml), Methanol (2x1 ml), DCM (2x1 ml) and DMF (2x1 ml) before coupling of the next amino acid. The following method was used for coupling of amino acid #2 (0.15 mmol), and was subsequently repeated for the couplings of amino acid #3 (0.15 mmol) and the capping carboxylic acid (0.40 mmol with 3.8 equiv. HATU). The 2CTC-resin was treated in a 3 mL syringe with a frit with a solution of amino acid #2 (0.15 mmol) and DIPEA (0.07 mL, 0.4 mmol, 4 equiv.) in DMF (0.6 ml). To this, was then aspirated a solution of HATU (72 mg, 0.19 mmol, 1.9 equiv.) in DMF (0.4 ml), and the corresponding solution was agitated at room temperature for 45 min, after which it was washed carefully with DMF (3x1 ml), Methanol (2x1 ml), DCM (2x1 ml) and DMF (2x1 ml). Following coupling of amino acids #2 or #3, removal of the Fmoc group was accomplished by treating the 2CTC resin with piperidine in Methanol (80%, 1 ml) for 20 min under agitation at room temperature. The reaction solution was then ejected from the syringe, and the 2CTC resin was carefully washed using DMF (3x1 ml), Methanol (2x1 ml), DCM (2x1 ml) and DMF (2x1 ml) before coupling of the next amino acid. After completed synthesis, the target peptides were cleaved from the 2CTC resin using a mixture of hexafluoroisopropanol/DCM (700 µl/300 µl), agitating for 10 minutes at room temperature. The crude materials were purified using reverse-phase chromatography (20-60% MeCN in H_2O, with 0.05% formic acid) over 8 CV with a flow of 30 mL/min.

Synthesis of Dabcyl-KTSAVLQSGFRKME-EDANS:

EDANS NovaTag™ resin (200 mg, 0.6 mmol/g) was pre-swelled in DMF. Fmoc-Glu-OH (3 eq.), HATU (3 eq.) and DIPEA (6 eq.) in DMF was thereafter added to the resin. The reaction mixture was gently agitated in an overhead shaker for 60 min. The resin was washed several times with DMF whereafter the Fmoc protection was removed with 4% DBU in DMF followed by washings with DMF, iPrOH, MeOH, H2O and DCM. The coupling procedure was repeated for the next coming Fmoc-amino acids in the following order: Fmoc-Met, Fmoc-Lys, Fmoc-Phe, Fmoc-Gly, Fmoc-Ser, Fmoc-Asn, Fmoc-Leu, Fmoc-Val, Fmoc-Ala, Fmoc-Ser, Foc-Thr and Fmoc Lys. In the final step Dabcyl was introduced by adding Dabcyl acid (3 eq.), HATU (3 eq.) and DIPEA (6 eq.) in DMF followed by agitation for 60 min. Final washing was done using DMF, iPrOH, MeOH, H2O and DCM. The final labeled peptide was cleaved from the resin using TFA:TES 95/5. The filtrate was collected and the crude product isolated by evaporation. The final product (purity 99%) was isolated after preparative HPLC purification using mobile phase: 0.1% TFA acetonitrile and 0.1% TFA in water (15–45%)

Acknowledgements

We would like to thank the Protein Science Facility (PSF) team at the Karolinska Institutet, for the production of recombinant SARS-CoV-2 main protease used in the enzymatic assays, Anders Olsson (SciLifeLab Stockholm) for the production of the recombinant Avi-tagged main protease used for the affinity screening of DECL, and Professor Stefan Sarafianos, and Grace Neilsen (Emory University) for kindly providing recombinant M^{pro} carrying the E166V variant. We also thank the Drug Discovery and Development platform (DDD, SciLifeLab) for providing access to the DELopen platform, Pawel Baranczewski for performing metabolic stability studies and Richard Svensson for performing cell permeability studies in Caco-2 cell lines.

Competing interests

The authors declare no competing interests.

Funding

Johan Lennerstrand was funded by the Scandinavian Society for Antimicrobial Chemotherapy (SLS-961049 and SLS-974118), Erik, Karin and Gösta Selander Foundation (2021 and 2022), and Knut and Alice Wallenberg Foundation and Science for Life Laboratory Uppsala (project “Nevermore Covid”).

References

1. Viana, R. *et al.* Rapid epidemic expansion of the SARS-CoV-2 Omicron variant in southern Africa. *Nature* **603**, 679–686 (2022).
2. Kurhade, C. *et al.* Low neutralization of SARS-CoV-2 Omicron BA.2.75.2, BQ.1.1 and XBB.1 by parental mRNA vaccine or a BA.5 bivalent booster. *Nat Med* 1–4 (2022) doi:10.1038/s41591-022-02162-x.
3. Lyke, K. E. *et al.* Rapid decline in vaccine-boosted neutralizing antibodies against SARS-CoV-2 Omicron variant. *Cell Reports Medicine* **3**, 100679 (2022).
4. Wang, Q. *et al.* Alarming antibody evasion properties of rising SARS-CoV-2 BQ and XBB subvariants. *Cell* **0**, (2022).

5. Keam, S. J. Tixagevimab + Cilgavimab: First Approval. *Drugs* **82**, 1001–1010 (2022).
6. Kim, J. Y. *et al.* A Randomized Clinical Trial of Regdanvimab in High-Risk Patients With Mild-to-Moderate Coronavirus Disease 2019. *Open Forum Infect Dis* **9**, ofac406 (2022).
7. Lee, S. *et al.* Regdanvimab in patients with mild-to-moderate SARS-CoV-2 infection: A propensity score-matched retrospective cohort study. *Int Immunopharmacol* **106**, 108570 (2022).
8. Zhang, L. *et al.* Crystal structure of SARS-CoV-2 main protease provides a basis for design of improved α-ketoamide inhibitors. *Science* **368**, 409–412 (2020).
9. V'kovski, P., Kratzel, A., Steiner, S., Stalder, H. & Thiel, V. Coronavirus biology and replication: implications for SARS-CoV-2. *Nat Rev Microbiol* **19**, 155–170 (2021).
10. Roe, M. K., Junod, N. A., Young, A. R., Beachboard, D. C. & Stobart, C. C. Targeting novel structural and functional features of coronavirus protease nsp5 (3CLpro, Mpro) in the age of COVID-19. *J Gen Virol* **102**, 001558 (2021).
11. Luttens, A. *et al.* Ultralarge Virtual Screening Identifies SARS-CoV-2 Main Protease Inhibitors with Broad-Spectrum Activity against Coronaviruses. *J. Am. Chem. Soc.* **144**, 2905–2920 (2022).
12. Owen, D. R. *et al.* An oral SARS-CoV-2 Mpro inhibitor clinical candidate for the treatment of COVID-19. *Science* **374**, 1586–1593 (2021).
13. Unoh, Y. *et al.* Discovery of S-217622, a Noncovalent Oral SARS-CoV-2 3CL Protease Inhibitor Clinical Candidate for Treating COVID-19. *J. Med. Chem.* **65**, 6499–6512 (2022).
14. Shionogi, press release. Xocova® (Ensitrelvir Fumaric Acid) Tablets 125mg Approved in Japan for the Treatment of SARS-CoV-2 Infection, under the Emergency Regulatory Approval System. https://www.shionogi.com/us/en/news/2022/11/xocova-ensitrelvir-fumaric-acid-tablets-125mg-approved-in-japan-for-the-treatment-of-sars-cov-2-infection,-under-the-emergency-regulatory-approval-system.html (2022).
15. Han, S. H. *et al.* Structure-Based Optimization of ML300-Derived, Noncovalent Inhibitors Targeting the Severe Acute Respiratory Syndrome Coronavirus 3CL Protease (SARS-CoV-2 3CLpro). *J. Med. Chem.* **65**, 2880–2904 (2022).
16. Huang, C. *et al.* A new generation Mpro inhibitor with potent activity against SARS-CoV-2 Omicron variants. *Sig Transduct Target Ther* **8**, 1–13 (2023).
17. Douangamath, A. *et al.* Crystallographic and electrophilic fragment screening of the SARS-CoV-2 main protease. *Nat Commun* **11**, 5047 (2020).
18. Chamakuri, S. *et al.* DNA-encoded chemistry technology yields expedient access to SARS-CoV-2 Mpro inhibitors. *Proceedings of the National Academy of Sciences* **118**, e2111172118 (2021).
19. Ge, R. *et al.* Discovery of SARS-CoV-2 main protease covalent inhibitors from a DNA-encoded library selection. *SLAS Discov* **27**, 79–85 (2022).
20. Satz, A. L. *et al.* DNA-encoded chemical libraries. *Nat Rev Methods Primers* **2**, 1–17 (2022).
21. Boras, B. *et al.* Preclinical characterization of an intravenous coronavirus 3CL protease inhibitor for the potential treatment of COVID19. *Nat Commun* **12**, 6055 (2021).
22. Hoffman, R. L. *et al.* Discovery of Ketone-Based Covalent Inhibitors of Coronavirus 3CL Proteases for the Potential Therapeutic Treatment of COVID-19. *J. Med. Chem.* **63**, 12725–12747 (2020).
23. Fu, L. *et al.* Both Boceprevir and GC376 efficaciously inhibit SARS-CoV-2 by targeting its main protease. *Nature Communications* **11**, 4417 (2020).
24. Qiao, J. *et al.* SARS-CoV-2 Mpro inhibitors with antiviral activity in a transgenic mouse model. *Science* **371**, 1374–1378 (2021).
25. MacDonald, E. A. *et al.* Recognition of Divergent Viral Substrates by the SARS-CoV-2 Main Protease. *ACS Infect. Dis.* **7**, 2591–2595 (2021).

27amilton, K. O., Backstrom, G., Yazdanian, M. A. & Audus, K. L. P-glycoprotein efflux pump expression and activity in Calu-3 cells. *J Pharm Sci* **90**, 647–658 (2001).

27. Iketani, S. *et al.* Multiple pathways for SARS-CoV-2 resistance to nirmatrelvir. *Nature* **613**, 558–564 (2023).
28. Lan, S. *et al.* Nirmatrelvir Resistance in SARS-CoV-2 Omicron_BA.1 and WA1 Replicons and Escape Strategies. 2022.12.31.522389 Preprint at https://doi.org/10.1101/2022.12.31.522389 (2023).
29. Zhou, Y. *et al.* Nirmatrelvir-resistant SARS-CoV-2 variants with high fitness in an infectious cell culture system. *Science Advances* **8**, eadd7197 (2022).
30. Akaberi, D. *et al.* Mitigation of the replication of SARS-CoV-2 by nitric oxide in vitro. *Redox Biology* **37**, 101734 (2020).
31. Ling, J. *et al.* Infectious SARS-CoV-2 is rarely present in the nasopharynx samples collected from Swedish hospitalized critically ill COVID-19 patients. *Ir J Med Sci* **192**, 227–229 (2023).
32. Corman, V. M. *et al.* Detection of 2019 novel coronavirus (2019-nCoV) by real-time RT-PCR. *Eurosurveillance* **25**, 2000045 (2020).

Supplementary material

Supplementary tables:

Supplementary table 1: Metabolic stability of SLL11 and SLL12

	Human liver microsomes		Mouse liver microsomes	
Compound	**In vitro half time (min)**	**Clint (µl/min/mg)**	**In vitro half time (min)**	**Clint (µl/min/mg)**
SLL11	10	139	9	154
SLL12	11	131	8	170

Supplementary figures:

Supplementary Figure 1: Avi-tagged SARS CoV-2 main protease efficiently immobilized to paramagnetic beads.

Immobilization of Mpro-Avi to paramagnetic streptavidin T1 beads was tested before DELopen selection. Mpro-Avi was efficiently captured to streptavidin T1 beads while no protein remained in the flowthrough or heated eluate samples, suggesting optimal target retention on beads during selection procedure.

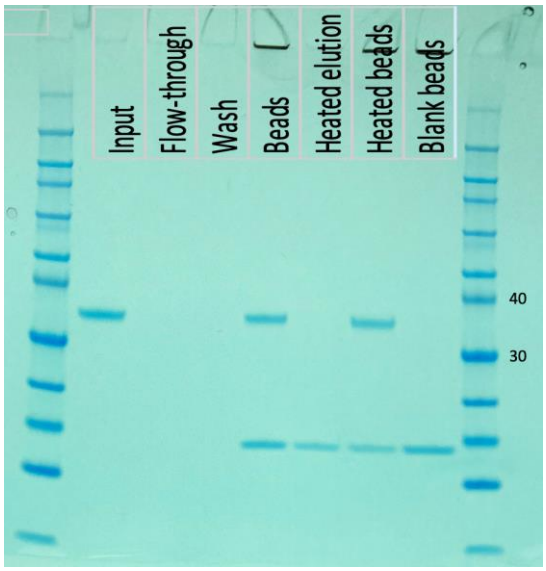

Supplementary Figure 1: Bead capture test of Mpro-Avi. Immobilization efficiency of C-terminally Avi-tagged Mpro to Streptavidin T1 beads (capture to 40 ul bead slurry). Capture efficiency deduced by comparing intensity of the input and flowthrough bands around 35 kDa. Absence of protein in heated elution lane confirms that there's no release of immobilized target upon heat denaturation. Markers of 30 and 40 kDa marked.

Supplementary Figure 2: Activity of avi-tagged Mpro coupled beads.

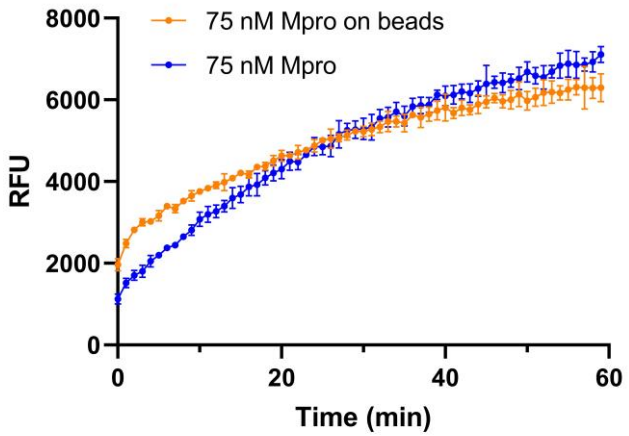

Supplementary Figure 2: Activity of Mpro enzyme on beads. The Mpro used for comparison of catalytic activity (at a final concentration of 75 nM) was obtained from the Protein Science Facility (PSF, Karolinska Institutet, Stockholm, Sweden). Mpro activity was analyzed by detection of hydrolysis of a quenched SARS-CoV-2 Mpro substrate (Bachem AG, Bubendorf, Switzerland). The assay was performed in 20 mM Tris, 50 mM NaCl and 0.1 mM EDTA (Merck KGaA, Darmstadt, Germany) at room temperature (pH 7.5) in Corning 3575 non-binding 384 well assay plates. Mpro, either in solution or on magnetic beads, was added to the assay plate using a 16-channel pipette (Integra ViaFlo, BergmanLabora AB, Sweden) and incubated for 15 minutes. Thereafter, the Mpro fluorogenic substrate (stock solution in 100% DMSO) was added to the assay plate to a final concentration of 10 µM, with a Labcyte ECHO 550 non-contact dispenser and fluorescence was measured at ambient temperature in kinetic mode every minute using a PerkinElmer Envision plate reader with excitation at 340 nm and emission at 490 nm.

Supplementary Figure 3: Off-target activity of compounds selected from DELopen.

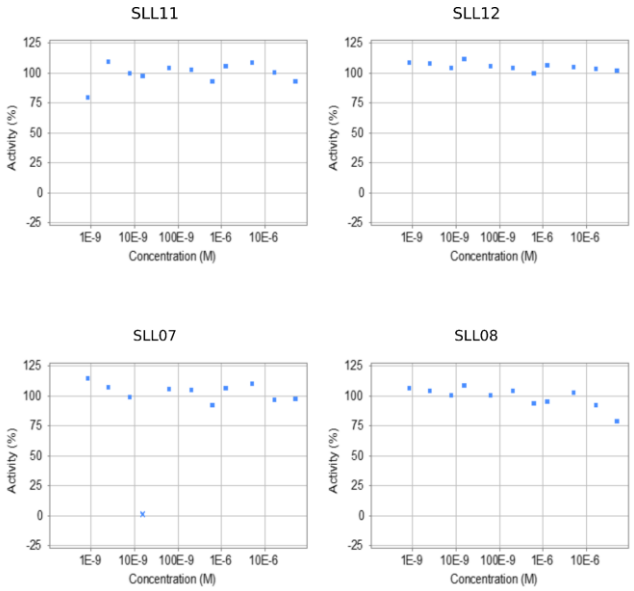

Supplementary Figure 3. Counter screening of compounds against human Cathepsin S enzymatic activity. Compounds SLL11, SLL12, SLL07 and SLL08 were tested at concentrations ranging from 50 to 0.00085 µM. At tested concentration no inhibitory activity was against Cathepsin S was observed.

Supplementary Figure 4: Dose response curves of compounds tested for the SAR study.

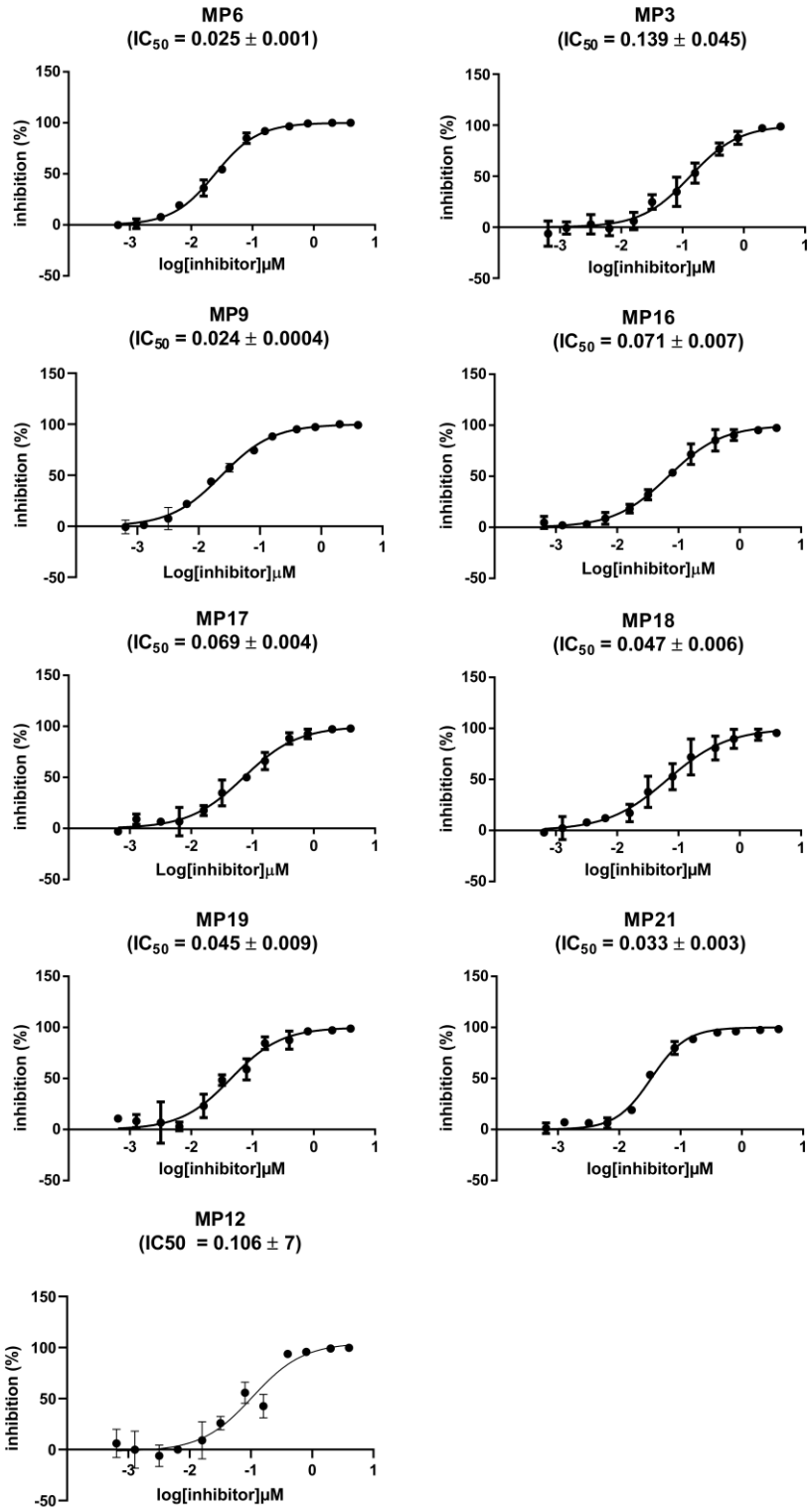

Supplementary Figure 4. Dose response curves and IC_{50} of compound MP6 and analogues that inhibited Mpro by 80% or more during the first screening performed at 1μM concentration. $IC50_s$ are reported as average from two independent experiments ± SEM.

Supplementary methods:

1.Expression and purification of SARS-CoV-2 3CL protease (for enzymatic assays)

SARS-CoV-2 3CL protease was produced by adopting a published construct used for the expression of SARS-CoV 3CL protease (Xue et al., 2007), containing nucleotide sequences corresponding to residues S1-Q306 (Chinese isolate, NCBI accession number YP_009725301). In this construct the 3CL protease is flanked by an N-GST (Glutathione S-transferases) tag and a C-HIS tag containing six histidine residues. The N-GST tag is cleaved directly by the SARS-CoV-2 protease thanks to the incorporation of the sequence of the N-terminus autocleavage site of SARS-CoV-2 3CL protease. While between the C-His tag and SARS-CoV-2 protease gene is present a cleavage site recognized by the Human rhinovirus 3C protease.

The vector (pGEX-6P-1) containing SARS-CoV-2 protease sequenced (kindly provided by Petra Lukacik, Frank von Delft and Martin Walsh) was transformed into *E. coli* BL21 (DE3)-T1R competent cells carrying the pRARE2 plasmid. A starter culture in L-Broth media (Formedium, Norfolk, UK) supplemented with carbenicillin (100 µg/ml) was inoculated from fresh transformants. The culture was grown at 37°C over the day until an OD_{600} of 1.5-2 was reached. The starter culture was then used to inoculate Auto Induction Media (AIM) Terrific Broth base with trace elements (Formedium, Norfolk, UK) supplemented with 1% glycerol and carbenicillin (100 µg/ml). When the OD_{600} reached 2, the cultures were shifted to 18 °C and the protein expression was continued overnight for 13 hours. Cells were harvested by centrifugation (10 min at 4500 × *g*, 4 °C), re-suspended in IMAC lysis buffer (50 mM Tris, 300 mM NaCl, pH 8.0) additionally containing Benzonase nuclease (10 µl/1.5 liter culture, 250 U/µl, E1014, Merck, Darmstadt, Germany), and disrupted by sonication (4s/4s 3 min, 80% amplitude, Sonics Vibracell-VCX750, Sonics & Materials Inc., Newtown, CT, US). Lysates were centrifuged at 49,000 × *g* for 20 min at 4 °C. The supernatants were filtered (Corning bottle-top vacuum filter, 0.45 µm, Corning, NY, USA) and imidazole was added to a final concentration of 10 mM before loading on the ÄKTA Xpress protein purification system (Cytiva, Little Chalfont, UK). Protein purification was performed using an IMAC HisTrap HP 5 ml column (Cytiva, Little Chalfont, UK). The column was washed with wash buffer (50 mM Tris, 300 mM NaCl, 25 mM imidazole, pH 8) and the bound protein was eluted with elution buffer (50 mM Tris, 300 mM NaCl, 500 mM imidazole, pH 8). The eluted protein was then treated with HRV 3C protease (1 µg/500 µg target protein, SAE0045, Merck, Darmstadt, Germany) in order to remove the C-His tag and the buffer was at the same time exchanged by dialysis (dialysis buffer 50 mM Tris, 300 mM NaCl, 0.5 mM TCEP and 0.5 mM DTT, pH 8) with a dialysis cassette (Slide-A-Lyzer Dialysis Cassette, 10K MWCO, 3mL, Thermo Fisher Scientific, Waltham, MA, USA) over night at 4 °C. Untagged SARS-CoV-2 3CL protease was purified by reverse IMAC purification using a HisTrap 1 ml column (Cytiva, Little Chalfont, UK), the same wash and elution buffers described above were used and the flow through was collected. The reverse IMAC purification was followed by a size exclusion chromatography step using a HiLoad 16/60 Superdex 200 preparative grade column (Cytiva, Little Chalfont, UK) equilibrated with gel filtration buffer (50 mM Tris, 300 mM NaCl, pH 8) and connected to a ÄKTA Express purification system. Fractions containing the target protein were examined by SDS PAGE, pooled together, concentrated with Vivaspin® 20 ml centrifugal concentrators (10 kDa MWCO, Sartorius, Goettingen, Germany) at 4000 × *g* and the buffer was at the same time exchanged to the final storage buffer (20 mM HEPES, 50 mM NaCl, pH 7.5). The protein was finally flash frozen in liquid nitrogen and stored at −80 °C.

2. Expression and Purification Protocol of Avi-tagged M^{pro} (for affinity selection of "DELopen" DNA encoded chemical library)

2.1-Construct details

Mpro was amplified with primers that would incorporate a C-terminal Avi-Tag, in place of the existing 6His tag. This was introduced into BamHI/XhoI cut pGEX-6P-1 by In-Fusion cloning. The resultant construct is GST-3C-✂Mpro-3C-AviTag, with the GST-3C portion being autocleaved by Mpro during expression (✂) and the terminal 3C site incorportaing the native C-terminal residues of Mpro. Purification is achieved by *in vivo* biotinylation during expression and a Streptavidin Mutein Matrix (Roche) pull down.

2.2-DNA sequence:

ATGTCCCCTATACTAGGTTATTGGAAAATTAAGGGCCTTGTGCAACCCACTCGACTTCTTTTGGAATATCTTGAA
GAAAAATATGAAGAGCATTTGTATGAGCGCGATGAAGGTGATAAATGGCGAAACAAAAAGTTTGAATTGGGTTT
GGAGTTTCCCAATCTTCCTTATTATATTGATGGTGATGTTAAATTAACACAGTCTATGGCCATCATACGTTATATAG
CTGACAAGCACAACATGTTGGGTGGTTGTCCAAAAGAGCGTGCAGAGATTTCAATGCTTGAAGGAGCGGTTT
TGGATATTAGATACGGTGTTTCGAGAATTGCATATAGTAAAGACTTTGAAACTCTCAAAGTTGATTTTCTTAGCAA
GCTACCTGAAATGCTGAAAATGTTCGAAGATCGTTTATGTCATAAAACATATTTAAATGGTGATCATGTAACCCAT
CCTGACTTCATGTTGTATGACGCTCTTGATGTTGTTTTATACATGGACCCAATGTGCCTGGATGCGTTCCCAAA
ATTAGTTTGTTTTAAAAAACGTATTGAAGCTATCCCACAAATTGATAAGTACTTGAAATCCAGCAAGTATATAGCA
TGGCCTTTGCAGGGCTGGCAAGCCACGTTTGGTGGTGGCGACCATCCTCCAAAATCGGATCTGGAAGTTCTG
TTCCAGGGGCCCCTGGGATCCGCTGTCTTACAGTCCGGTTTCCGTAAGATGGCCTTCCCGTCAGGCAAAGTG
GAAGGCTGTATGGTGCAAGTAACGTGCGGGACCACAACGTTGAACGGTTTGTGGTTAGATGATGTGGTTTACT
GTCCACGTCATGTTATCTGTACAAGTGAGGACATGCTTAATCCAAATTATGAGGACTTGTTGATCCGCAAAAGC
AACCATAATTTCCTGGTACAGGCAGGCAACGTTCAGTTACGTGTCATTGGTCATTCAATGCAAAACTGCGTGTT
GAAGCTGAAAGTAGATACAGCCAACCCGAAAACCCCGAAATATAAATTTGTCCGTATTCAGCCAGGCCAGACC
TTTTCGGTTCTGGCGTGCTACAACGGTAGCCCATCTGGGGTCTACCAGTGCGCTATGCGTCCTAACTTTACAA
TTAAGGGCAGTTTCTTGAACGGTAGCTGCGGAAGCGTTGGCTTTAATATTGACTACGATTGTGTGTCATTTTGC
TATATGCACCACATGGAGTTACCCACTGGAGTTCACGCGGGAACTGACCTGGAGGGGAACTTCTATGGGCCA
TTTGTGGATCGCCAGACGGCGCAGGCGGCCGGAACGGATACTACTATTACCGTGAATGTCCTTGCTTGGTTAT
ACGCGGCCGTCATTAACGGTGACCGTTGGTTTTTAAACCGTTTCACCACGACCCTTAATGATTTTAATTTGGTG
GCTATGAAGTATAACTACGAACCCCTGACGCAGGACCACGTAGATATTTTGGGGCCGCTGTCGGCACAGACG
GGAATTGCAGTGTTAGATATGTGTGCTTCATTGAAAGAGTTGTTACAGAACGGTATGAATGGACGCACAATTTT
GGGATCAGCATTATTAGAGGATGAGTTTACTCCGTTTGATGTTGTGCGTCAGTGCTCGGGTGTAACTTTCCAG
GGGCCGGGCCTGAATGATATTTTCGAGGCACAGAAAATTGAATGGCATGAGTGA

2.3-Protein sequence:

MSPILGYWKIKGLVQPTRLLLEYLEEKYEEHLYERDEGDKWRNKKFELGLEFPNLPYYIDGDVKLTQSMAIIRYIADK
HNMLGGCPKERAEISMLEGAVLDIRYGVSRIAYSKDFETLKVDFLSKLPEMLKMFEDRLCHKTYLNGDHVTHPDFM
LYDALDVVLYMDPMCLDAFPKLVCFKKRIEAIPQIDKYLKSSKYIAWPLQGWQATFGGGDHPPKSDLEVLFQGPLG
SAVLQ✂SGFRKMAFPSGKVEGCMVQVTCGTTTLNGLWLDDVVYCPRHVICTSEDMLNPNYEDLLIRKSNHNFLV
QAGNVQLRVIGHSMQNCVLKLKVDTANPKTPKYKFVRIQPGQTFSVLACYNGSPSGVYQCAMRPNFTIKGSFLNG
SCGSVGFNIDYDCVSFCYMHHMELPTGVHAGTDLEGNFYGPFVDRQTAQAAGTDTTITVNVLAWLYAAVINGDR
WFLNRFTTTLNDFNLVAMKYNYEPLTQDHVDILGPLSAQTGIAVLDMCASLKELLQNGMNGRTILGSALLEDEFTPF
DVVRQCSGVTFQGPGLNDIFEAQKIEWHE

GST, 3C sites, Mpro,Mpro autocleavage site (✂), Avi-Tag

2.4- Expression method:

Expression Strain:

Rosetta-BirA: BL21(DE3)-pRARE-2-pCDF-BirA (Chl/Strep)

AIM TB medium:

55.85 g Formedium AIM TB, including trace elements

10 mL glycerol

Topped up to 1 L with MilliQ water

Autoclaved to sterilise.

10 mM Biotin:

For each litre of culture 48.8 mg D-Biotin (IBA-LifeSciences) were weighed out and made up to 20 mL with 10 mM Bicine, pH 8.3, buffer (pre-heated for 30 seconds at full power in the microwave). This was vortexed to fully dissolve the Biotin and then filtered through a 0.22 µm syringe filter to sterilise.

Growth conditions:

A streak of colonies from each Rosetta-BirA transformation plate was inoculated into 1 mL LB medium, containing 100 µg/mL carbencillin and 50 µg/mL Streptomycin, and grown at 37°C 650 rpm for 1 hour. This was then inoculated into 10 mL LB, containing 100 µg/mL carbencillin and 50 µg/mL Streptomycin, and grown at 37°C 200 rpm for a further 2 hours. This was finally inoculated into 100 mL LB medium, containing 100 µg/mL carbencillin and 50 µg/mL Streptomycin, and grown at 37°C 200 rpm for 5 hours. Finally 10 mL of the starter culture were inoculated into each 2.5 L baffled flask of pre-warmed 1 L AIM TB, containing 100 µg/mL carbenicillin, 50 µg/mL Streptomycin and 20 mL of 10 mM Biotin solution. This was grown at 37°C 200 rpm for 5 hours at which point the temperature was reduced to 18°C overnight. The cells were harvested by centrifugation at 4,500 rpm for 30 minutes at 4°C.

2.5-Purification:

Buffers:

Lysis Buffer: 50 mM Tris, pH 8.0
300 mM NaCl

Elution Buffer 1: 50 mM Tris, pH 8.0
300 mM NaCl
10 mM Biotin

Elution Buffer 2: 50 mM Tris, pH 8.0
300 mM NaCl
50 mM Biotin

(+26 mM NaOH (130 µL 10 mM NaOH per 50 mL) to get Biotin into solution)

Mutein Wash Buffer: 100 mM potassium phosphate buffer, pH 7.2
150 mM NaCl

Mutein Equilibration Buffer: 100 mM potassium phosphate buffer, pH 7.2
150 mM NaCl
400 mM Ammonium sulfate

50% Streptavidin Mutein Matrix: Streptavidin Mutein Matrix (Roche)
Washed twice with Mutein Wash Buffer

Washed three times in Mutein Equilibration Buffer

Resuspended to 50% in Mutein Equilibration Buffer

Purification protocol:

A 1L pellet (~25 g cells) was thawed at room temperature and decanted into a beaker.

Lysis Buffer was added at a ratio of 30 mL per 10 g of cells and supplemented with 3 µg Benzonase (do not add protease inhibitors). This was stirred at 4 °C until the cell pellet had fully resuspended.

The cells were lysed by sonication for 5 minutes on ice, with 15 seconds on and 15 seconds off (a cell disruptor may also be used).

The lysate was decanted into 50 mL JA 25.50 centrifuge tubes and centrifuged for 1 hour at 50,000 xg.

The cleared lysate was carefully decanted off into 50 mL falcon tubes and a total of 5 mL (bed volume) of the Streptavidin Mutein Matrix split across the tubes. These were then placed on a rotary mixer for 1 hour at 4°C.

The mixture was transferred into a BioRad Econo-Column, the flow-through discarded.

The resin was washed 3 times with 40 mL Lysis Buffer.

5 mL of Elution Buffer 1 were applied and incubated for 10 minutes before eluting.

The remainder of the protein was then eluted with another 5 mL of Elution Buffer 1 and two additions of Elution Buffer 2.

The elutions were analysed by SDS-PAGE (example shown below) and the appropriate fractions pooled.

The sample was concentrated down to 5 mL using an Amicon Ultra-15 10 kDa MWCO concentrator, passed through a 0.22 um filter onto an S200 16/60 HiLoad Gel Filtration column run in Lysis Buffer. This step removes the Biotin and contaminating GST only band.

The GFC fractions were analysed by SDS-PAGE, appropriate fractions pooled (Mpro runs as a dimer) and concentrated to the desired final concentration before snap freezing in liquid nitrogen.